ECS Journal of Solid State
Science and Technology

Spray-Deposited Al_2O_3 for Rear Passivation and Optical Trapping in Silicon Solar Cells

Spray-Deposited Al_2O_3 for Rear Passivation and Optical Trapping in Silicon Solar Cells

Woo Jung Shin,[1,z] Wen-Hsi Huang,[1] and Meng Tao[2,*,z]

[1] *School for Engineering of Matter, Transport and Energy, Arizona State University, Tempe, Arizona 85287, USA*
[2] *School of Electrical, Computer and Energy Engineering, Arizona State University, Tempe, Arizona 85287, USA*

Low-cost spray deposition is employed to investigate the suitability of spray-deposited Al_2O_3 for rear passivation and optical trapping in passivated emitter rear contact (PERC) Si solar cells. Structural, optical, and electrical properties of spray-deposited Al_2O_3 films are investigated. Capacitance-voltage measurements indicate that spray-deposited Al_2O_3 has a negative charge density of 3.19×10^{12} cm^{-2} for an 80-nm film, suggesting that it can serve as the passivation layer. Optical properties of spray-deposited Al_2O_3 are identical to the Al_2O_3/SiN_x stack prepared by atomic layer deposition and plasma-enhanced chemical vapor deposition, indicating that it can also serve as the optical trapping layer. Atomic force microscopy studies show that spray-deposited Al_2O_3 is crack and pore free, and its surface roughness has a root-mean-square value of 0.52 nm for an 80-nm film. Spray-deposited Al_2O_3 is amorphous as determined by X-ray diffraction. X-ray photoelectron spectroscopy analysis suggests that spray-deposited Al_2O_3 is slightly Al-rich. The resistivity and breakdown field of an 80-nm Al_2O_3 film are 5.46×10^{14} Ω-cm and 3.28 MV/cm, respectively, which are stable after 800°C firing. These properties suggest that spray-deposited Al_2O_3 is a promising candidate to replace the Al_2O_3/SiN_x stack in Si PERC cells.

 [DOI: 10.1149/2.0211910jss]

Manuscript submitted April 9, 2019; revised manuscript received September 29, 2019. Published October 10, 2019.

The solar photovoltaic industry has been dominated by the Al back-surface field (BSF) cell for many years. However, the Al BSF technology is approaching its practical limit, and further gains in efficiency are unlikely. The search for continued efficiency improvements has led to the adoption of the passivated emitter rear contact (PERC) cell which offers a 1% absolute gain in efficiency by integrating a localized BSF structure.[1] As of 2016, PERC cells accounted for 15% of the global Si solar cell production and they are expected to become the dominant cell technology in the near future.[2] In PERC cells, a thin layer of Al_2O_3, about 10 nm, is deposited on the rear of the Si cell, which reduces rear surface recombination on p-type Si by chemical and field-effect passivation.[3] The 10-nm Al_2O_3 film is supported by an 80–150 nm SiN_x capping layer. The low refractive index of SiN_x improves light trapping by rear reflection.[4] It also prevents Al etching of the Al_2O_3 film during the high-temperature firing process.[5]

Al_2O_3 films are typically synthesized by vacuum-based processes such as atomic layer deposition (ALD),[6] plasma-enhanced chemical vapor deposition (PECVD),[7] metal organic chemical vapor deposition,[8] and sputter deposition.[9] For commercial Si PERC cells, the Al_2O_3 film is prepared by ALD. ALD is a slow process and the precursor for Al_2O_3, $Al_2(CH_3)_6$, is expansive and pyrophoric. For these reasons the thickness of the Al_2O_3 film in Si PERC cells is limited to about 10 nm and an 80–150 nm SiN_x layer is deposited on Al_2O_3 by PECVD to provide rear reflection and protection for Al_2O_3 as shown in Fig 1a. It is noted that the refractive index of Al_2O_3 is lower than that of SiN_x, 1.6 vs. 2.0,[6,10] so a thicker Al_2O_3 film on the rear of the PERC cell as shown in Fig 1b should provide better optical trapping than an Al_2O_3/SiN_x stack. This requires a low-cost process to deposit thicker Al_2O_3 on Si and verification of the passivation effect and thermal stability of thicker Al_2O_3.

Low-cost processes such as sol-gel deposition[11] or spray deposition[12] have been explored for Al_2O_3. However, those studies used high-temperature processes (850°C in O_2) or toxic and expensive solvents such as 2-methoxyethanol. Since spray pyrolysis is a continuous, open-air process, the use of organic solvents at high temperatures introduces potential fire and explosion risks in mass production. In this paper, we report successful Al_2O_3 deposition on Si by spray pyrolysis using water as the solvent, which ensures a lower cost and safer process. Optical, electrical, and structural properties of spray-deposited Al_2O_3 are investigated and compared to the industrial standard ALD Al_2O_3/PECVD SiN_x stack, to reveal the suitability of spray-deposited Al_2O_3 for rear passivation and optical trapping in Si PERC cells.

Experimental

Amorphous Al_2O_3 films were obtained by spray deposition in air. The precursor solution was prepared with 0.1 M Al acetylacetonate ($Al(C_5H_7O_2)_3$) and 0.2 M HCl in water. It is noted that although the price of the ALD precursor, $Al_2(CH_3)_6$, has been declining, it is still significantly more expensive than the spray deposition precursor, $Al(C_5H_7O_2)_3$. HCl was added to completely dissolve the Al precursor in the solution. The Si wafers used in this work were textured p-type Czochralski (CZ) (100) wafers of 2 Ω-cm. The thickness of the wafers was 200 μm and they were cut into pieces of 4×4 cm^2. Si substrates were cleaned with diluted HF to remove native oxide from the surface before spray deposition. The starting Si substrates had a minority carrier lifetime of 20 μs after HF dip. The substrate was placed on a hotplate and the temperature of the hotplate was set between 400°C and the highest temperature of the hotplate, 550°C. In order to reduce the fluctuations in substrate temperature and provide ample time for solvent evaporation, pulsed spray deposition was employed with each cycle comprised of 10 s on and 50 s off.[13] The optimized deposition parameters for Al_2O_3 are listed in Table I.

For a comparative study, 10-nm ALD Al_2O_3 and 80-nm PECVD SiN_x were deposited sequentially on Si substrates using $Al_2(CH_3)_6$ and a mixture of SiH_4 and NH_3 as the precursors, respectively. The deposition temperature was 200°C for both ALD Al_2O_3 and PECVD SiN_x. Optical and electrical properties of the Al_2O_3/SiN_x stack were measured and compared with those of spray deposited Al_2O_3.

Capacitance-voltage (C-V) measurements were performed using a MDC C-V system with a Hg probe. For current-voltage (I-V) characterization, a MDC probe station equipped with a HP 4140B current meter was used. The refractive index of Al_2O_3 films was measured

Table I. Optimized parameters for spray deposition of Al_2O_3 films on Si.

Nozzle-substrate distance (cm)	65
Al concentration (M)	0.1
Solution flow rate (ml/min)	17
Carrier gas	Air
Atomization/piston pressure (pa)	35/40

*Electrochemical Society Member.
[z]E-mail: meng.tao@asu.edu; wshin4@asu.edu

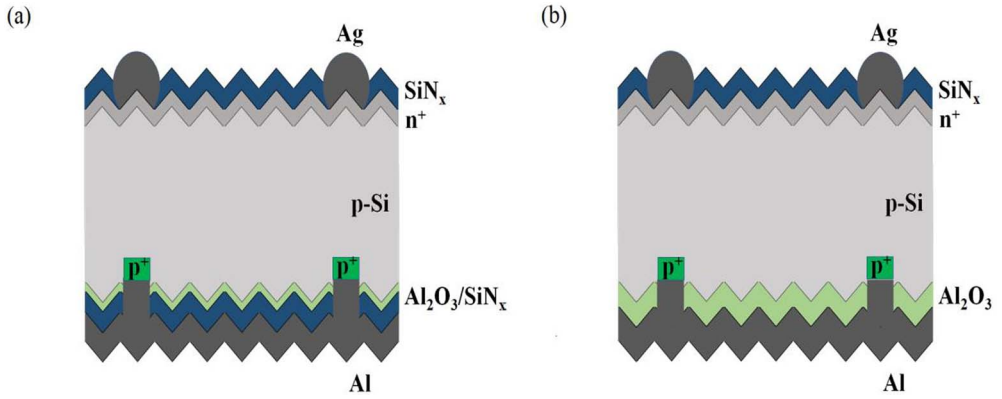

Figure 1. Schematic structure of the p-type Si PERC cell with a (a) 10-nm Al_2O_3/80-nm SiN_x stack and (b) thicker Al_2O_3 layer on the rear.

with a Woollam VASE ellipsometer. Optical properties of Al_2O_3 films were characterized with a JASCO V-670 spectrophotometer. X-ray diffraction (XRD) spectra were obtained using a Panalytical X-ray diffractometer under grazing incident angles. Surface roughness of the films was measured by a Park System atomic force microscope (AFM). The thickness of Al_2O_3 films on textured Si substrates was analyzed using a Hitachi S4700 field-emission scanning electron microscope (SEM). Elemental analysis was carried out with a VG 220i-XL X-ray photoelectron spectrometer. The minority carrier lifetime was measured with a Sinton WCT-120 lifetime tester in the quasi-steady-state photoconductance mode.

Results and Discussion

The first experiment carried out was the optimization of the spray deposition parameters for Al_2O_3. The minority carrier lifetime of Si substrates covered with Al_2O_3 on both sides was monitored for this experiment. As shown in Fig 2, the minority carrier lifetime strongly

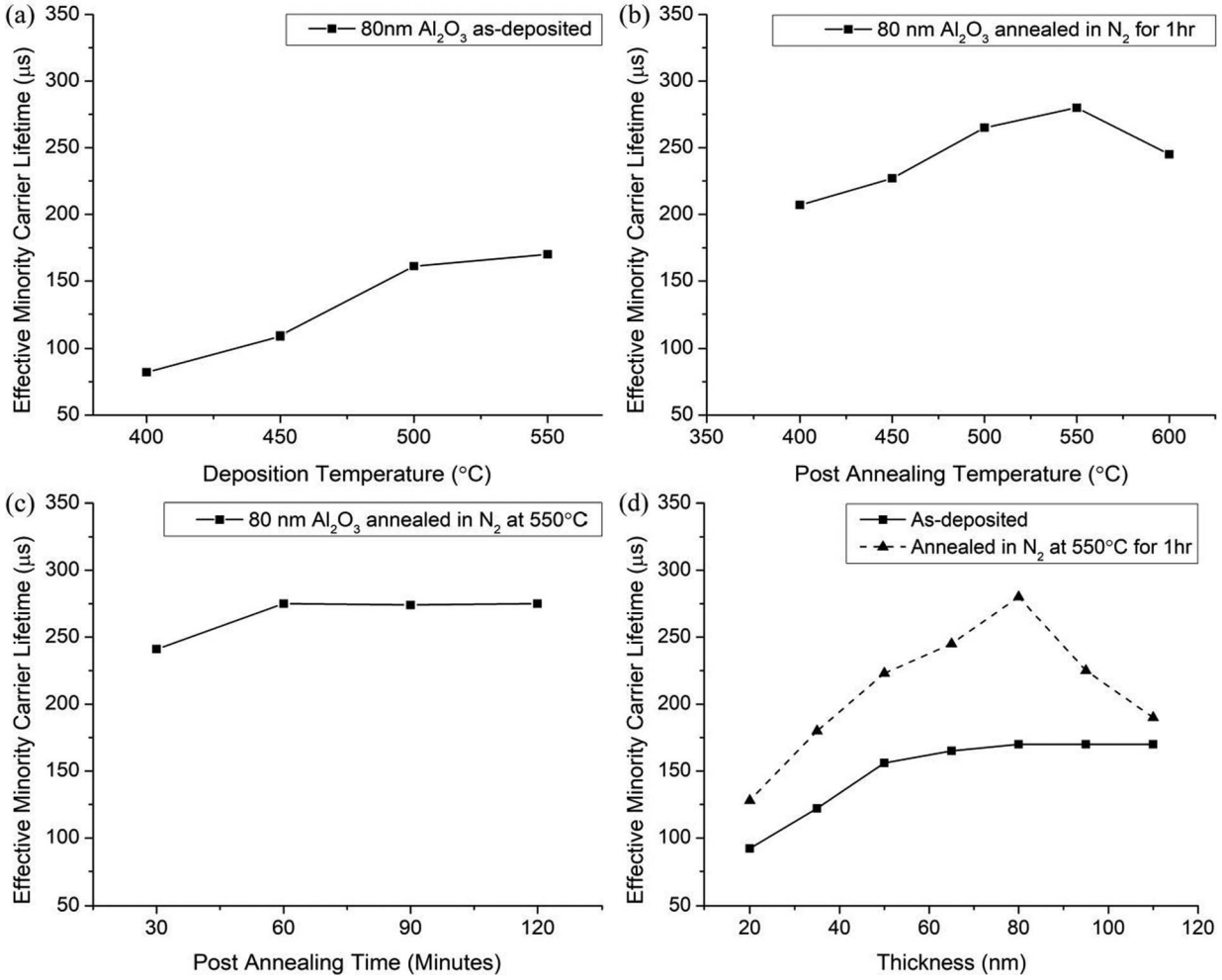

Figure 2. Minority carrier lifetime of p-type Si covered by Al_2O_3 on both sides at different (a) deposition temperatures, (b) post-annealing temperatures, (c) post-annealing times, and (d) Al_2O_3 thicknesses.

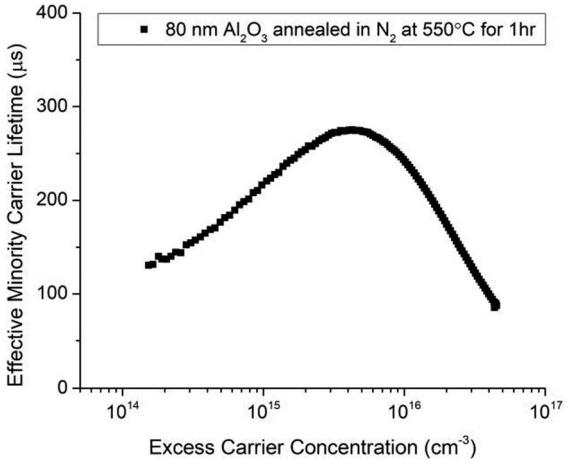

Figure 3. Minority carrier lifetime as a function of excess carrier concentration. The lifetime was measured on a Si sample covered with Al_2O_3 using the optimized deposition parameters.

depends on deposition parameters such as deposition temperature, Al_2O_3 thickness, and post-annealing conditions. Fig. 2a presents the effect of deposition temperature on minority carrier lifetime. The thickness of Al_2O_3 was fixed to 80 nm. The lifetime increases linearly with deposition temperature from 400°C to 550°C, and 550°C is the highest temperature the hotplate can reach. The minority carrier lifetime is 170 μs at 550°C, while the starting substrate has a lifetime of 20 μs. Samples prepared at 550°C were post-annealed in N_2 at different conditions to further improve the minority carrier lifetime. Fig. 2b compares the minority carrier lifetime of Si with 80-nm Al_2O_3 at different post-annealing temperatures for 1 hr. The lifetime increases from 205 μs to 280 μs with post-annealing temperature from 400°C to 550°C. At 600°C, the lifetime decreases. Fig. 2c shows the effect of post-annealing time on minority carrier lifetime. The post-annealing temperature and the thickness of Al_2O_3 were fixed to 550°C and 80 nm, respectively. The lifetime increases from 234 μs to 280 μs with annealing time from 30 min to 1 hr. Further increase in annealing time above 1 hr does not result in a higher lifetime. Fig. 2d illustrates the effect of Al_2O_3 thickness on minority carrier lifetime. The lifetime was measured before and after post annealing in N_2 at 550°C for 1 hr. In both cases, the maximum lifetime was obtained with 80-nm Al_2O_3.

From the experiment described above, the best deposition parameters were identified as: deposition temperature 550°C, Al_2O_3 thickness 80 nm, post-annealing temperature 550°C, and post-annealing time 1 hr. These parameters were used in all the following experiments.

Fig. 3 shows the minority carrier lifetime for a Si sample as a function of excess carrier concentration. The Si sample was covered with Al_2O_3 on both sides using the optimized deposition parameters described above. A lifetime of 280 μs is obtained at the excess carrier concentration of 4×10^{15} cm^{-3}. From the measured minority carrier lifetime, the surface recombination velocity, S_{eff}, is calculated using the following equation:[14]

$$\frac{1}{\tau_{eff}} = \frac{1}{\tau_{bulk}} + \frac{1}{W/2S_{eff} + W^2/\left(D_n\pi^2\right)} \quad [1]$$

where τ_{bulk} is the bulk lifetime of the substrate, W and D_n are the thickness and electron diffusion coefficient of the substrate, respectively. S_{eff} was calculated assuming an infinite bulk lifetime and D_n = 29.82 cm^2/s for Si substrates of 2 Ω-cm.[15] A S_{eff} value of 35.89 cm/s is obtained for the sample with 80-nm Al_2O_3 on both sides after post annealing at 550°C for 1 hr.

The thickness of Al_2O_3 films on Si substrates was measured using both destructive and non-destructive methods as shown in Figs. 4 and 5. Fig. 4 shows SEM cross-sectional images of Al_2O_3 deposited on polished and textured Si substrates. As shown in Fig. 4a, the Al_2O_3 film deposited on a polished substrate shows a uniform and smooth morphology of 80 nm. However, the Al_2O_3 film deposited with the same parameters on a textured substrate shows thickness variations over the pyramidal surface due to shadowing effects caused by the pyramids. Fig. 4b is the SEM cross-sectional image of a sample with a lifetime of 280 μs. The thickness on top of a pyramid is about 135 nm, but it reduces to about 55 nm between pyramids. Since passivation quality strongly depends on the thickness of the Al_2O_3 layer as shown in Fig. 2d, it is predicted that improvement in film thickness uniformity should enhance the passivation quality of Al_2O_3 on p-type Si.

Due to thickness non-uniformity on textured substrates, the average thickness of Al_2O_3 was measured using the refractive index and reflectance spectrum of Al_2O_3 as presented in Fig. 5. For a transparent film with a refractive index n, its thickness d can be calculated by:[16]

$$d = \lambda/4n \quad [2]$$

where λ is the minimum in the reflectance spectrum. Fig. 5a shows the reflectance spectrum of Al_2O_3 on textured Si. The optimized deposition parameters for a minority carrier lifetime of 280 μs were used to prepare the Al_2O_3 film on one side of the textured Si substrate. The minimum reflectance of 3.2% was found at the wavelength of 513 nm. At this wavelength, the corresponding refractive index of Al_2O_3 was measured to be 1.61 as shown in Fig. 5b. Therefore, the average thickness of the Al_2O_3 film which resulted in the highest lifetime of 280 μs was calculated to be 79.65 nm, very close to the nominal thickness of 80 nm.

Fig. 6 shows the C-V characteristics of 80-nm Al_2O_3 on Si substrates measured at a frequency of 100 kHz using the retrace mode. The substrates for C-V were p-type polished CZ Si(100) wafers of

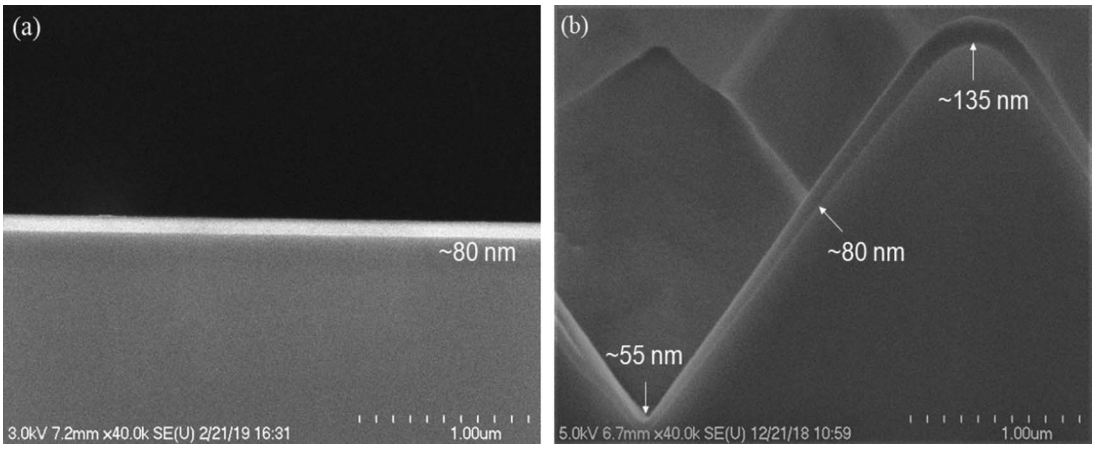

Figure 4. SEM cross-sectional images of Al_2O_3 films deposited on (a) polished and (b) textured Si(100) substrates.

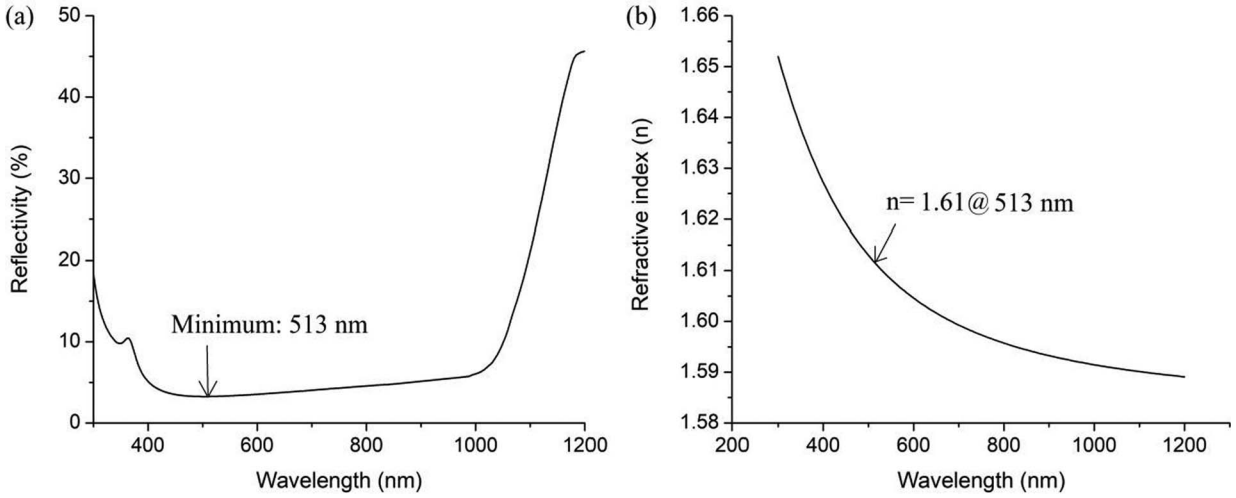

Figure 5. (a) Reflectance spectrum of textured Si covered with 80-nm Al_2O_3 on one side and (b) refractive index of 80-nm Al_2O_3 on textured Si.

0.5 Ω-cm. Fig. 6a presents the C-V curve of a 80-nm Al_2O_3/Si sample after post annealing in N_2 at 550°C for 1 hr. The oxide capacitance of 410 pF translates into a dielectric constant of 8.1 for spray-deposited Al_2O_3 which was calculated from the contact area of the Hg probe (0.456 mm^2) and the oxide thickness (80 nm). This value is close to Al_2O_3 prepared by ALD.[6] The flat-band voltage and density of fixed charges in 80-nm Al_2O_3 were calculated to be +5.5 V and –3.19 $\times$ 10^{12} cm^{-2}, respectively. The density of negative fixed charges in 80-nm spray-deposited Al_2O_3 is low compared to 45-nm ALD Al_2O_3 (10^{13} cm^{-2}),[17] which is likely due to improved stoichiometry and fewer structural defects in spray-deposited Al_2O_3 than ALD Al_2O_3. Our spray-deposited Al_2O_3 is obtained at a higher deposition temperature, 550°C vs. 200°C for ALD, and with an ample supply of oxygen from the solvent, water.

Fig. 6b reveals that the C-V curve at 450°C shifts to the left as compared the C-V curve at 550°C, indicating a lower density of negative fixed charges in the 450°C film. In addition, a hysteresis exists in the 450°C C-V curve revealing the existence of slow charges associated with defects. This suggests that the lower lifetime for lower deposition temperatures below 550°C in Fig. 2a is likely due to the combined effect of a lower density of fixed charges and a higher density of interfacial defects. The defects are introduced by lower thermal energy provided to Al atoms at lower deposition temperatures. Moreover, the C-V curves at 450°C and 550°C both show a small hump which is characteristic of interfacial defects.[18] This hump disappears completely upon post annealing in N_2 (Fig. 6a). There is no flat-band voltage shift between 550°C as-deposited and post-annealed samples indicating that the improved lifetime after post annealing in Fig. 2b is likely caused by reduced interfacial defects, not by an increase in negative charge density. It is possible that with 550°C post-annealing, SiO_2 forms at the interface between Al_2O_3 and Si resulting in a lower density of interfacial defects as this has been observed in high-k/Si interfaces after high-temperature annealing. The interfacial defect density after 550°C annealing is in the 10^{11} cm^{-2} range.

To compare light trapping between spray-deposited Al_2O_3 films and the industrial standard Al_2O_3/SiN_x stack for Si PERC cells, Al_2O_3 of different thicknesses was spray-deposited on the rear of textured Si substrates and compared to a sample with a 10-nm ALD Al_2O_3/80-nm PECVD SiN_x stack on the rear. 250 nm Al was deposited by electron-beam evaporation on spray-deposited Al_2O_3 and ALD Al_2O_3/PECVD SiN_x to mimic the rear Al electrode in PERC cells. On the front side of the samples, 75-nm PECVD SiN_x was deposited as the anti-reflection layer. Reflectance spectra were measured for these samples between 300 nm and 1,112 nm, the latter being the cutoff wavelength for Si at the typical operating temperature of Si solar cells, 48°C. Fig. 7a shows the reflectance spectra of the samples with different thicknesses of spray-deposited Al_2O_3. There is little difference in reflectance between 300 nm and 1,000 nm, but the reflectance above 1,000 nm increases

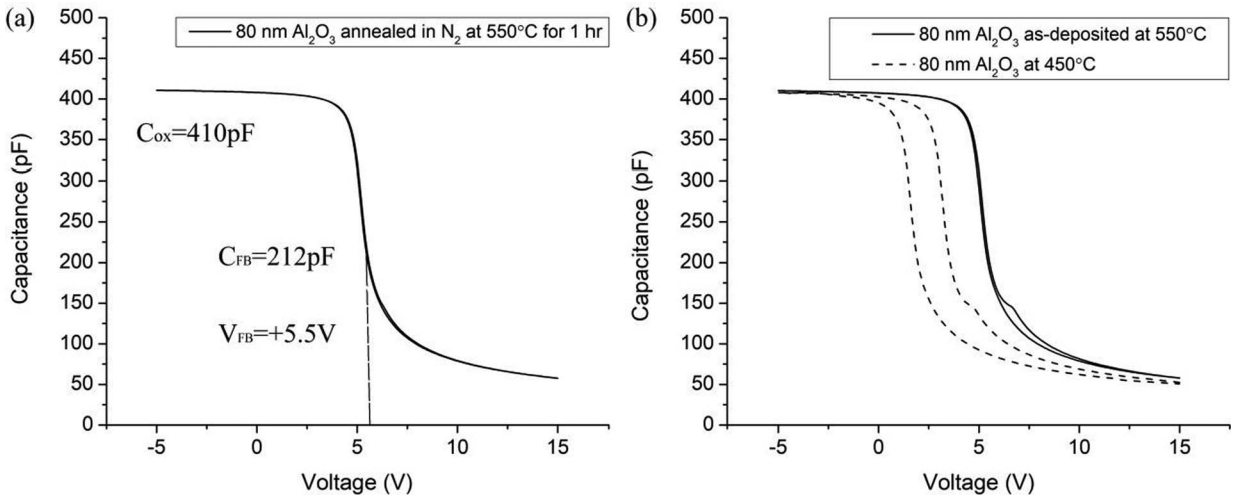

Figure 6. C-V characteristics of 80-nm Al_2O_3 deposited at (a) 550°C followed by post annealing in N_2 at 550°C for 1 hr and (b) 450°C and 550°C without post annealing.

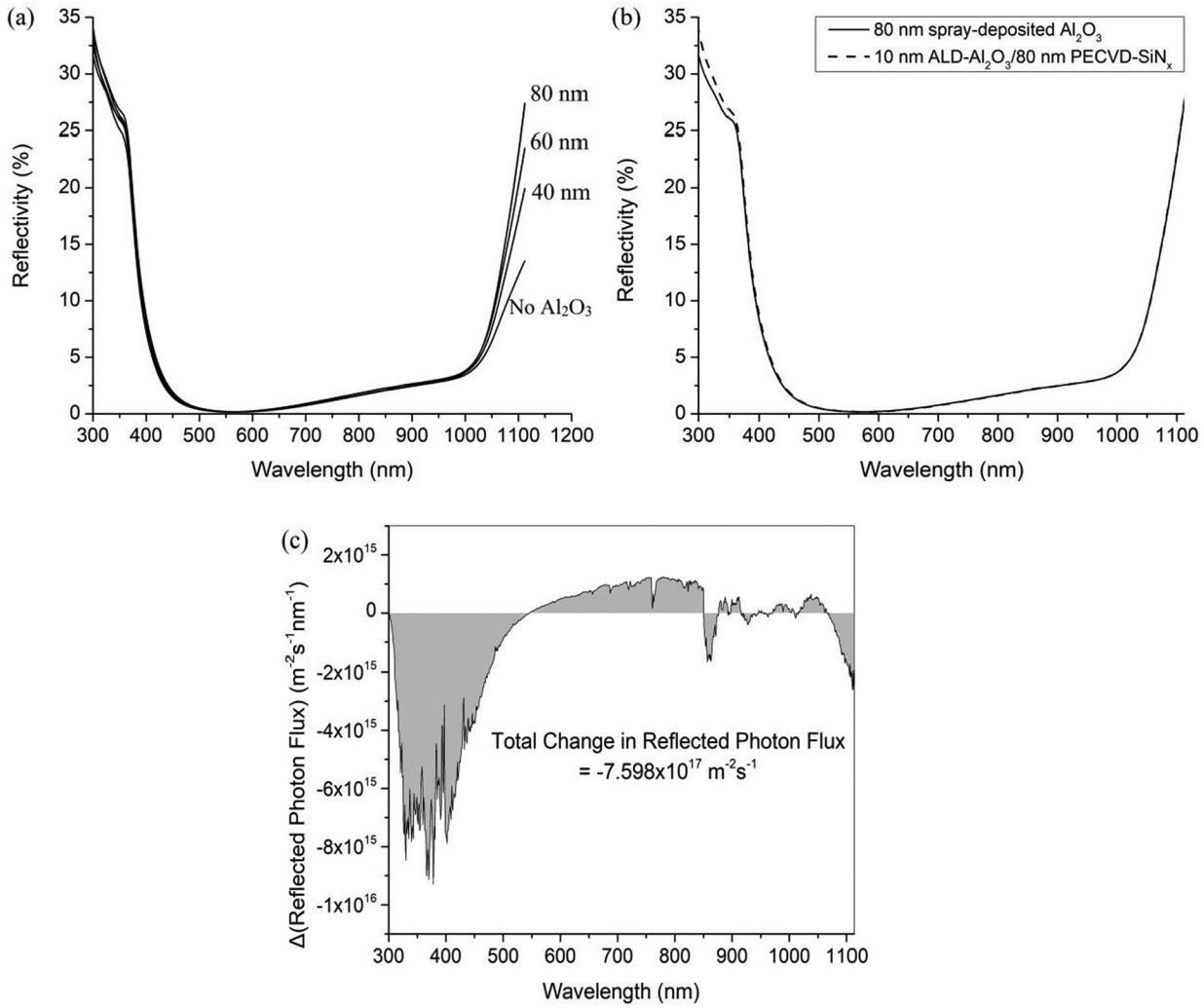

Figure 7. (a) Reflectance spectra of Al_2O_3 with different thicknesses on the rear of Si substrates. (b) Reflectance spectra of 80-nm spray-deposited Al_2O_3 and 10-nm ALD Al_2O_3/80-nm PECVD SiN_x. (c) Change in reflected photon flux between 80-nm Al_2O_3 and 10-nm Al_2O_3/80-nm SiN_x as a function of wavelength.

with the thickness of spray-deposited Al_2O_3. Fig. 7b compares the reflectance spectra of 80-nm spray-deposited Al_2O_3 with a 10-nm ALD Al_2O_3/80-nm PECVD SiN_x stack. The two reflectance spectra are almost identical.

With the incident photon flux at AM1.5 as a function of wavelength, the difference in reflected photon flux between an 80-nm spray-deposited Al_2O_3 film and a 10-nm ALD Al_2O_3/80-nm PECVD SiN_x stack was calculated by multiplying the change in reflectance with the incident photon flux at each wavelength:[13]

$$\Delta\Phi_{Reflected}(\lambda) = [(R_{Al_2O_3}(\lambda) - R_{Al_2O_3/SiN_x}(\lambda)] \times \Phi_{Incident}(\lambda) \quad [3]$$

As shown in Fig. 7c, negative values indicate that 80-nm spray-deposited Al_2O_3 reflects less than the ALD Al_2O_3/PECVD SiN_x stack. Integrating the change in reflected photon flux over wavelength reveals that spray-deposited Al_2O_3 reflects a net of 7.598×10^{17} $m^{-2}s^{-1}$ fewer photons than the ALD Al_2O_3/PECVD SiN_x stack. This is less than 0.03% of the total number of photons in the AM1.5 solar spectrum with energy above the Si bandgap, which is within the margin of error. Therefore, spray-deposited Al_2O_3 is optically identical to ALD Al_2O_3/PECVD SiN_x stack as the rear reflector in Si PERC cells.

Fig. 8a shows a XRD spectrum of a 500-nm Al_2O_3 film after post annealing at 550°C. No diffraction peaks over the entire range of two theta indicate that spray-deposited Al_2O_3 under the optimized deposition parameters is amorphous. Fig. 8b is an AFM scan of an 80-nm Al_2O_3 film on a polished CZ Si(100) substrate after post annealing at 550°C. The scan area is 9×9 μm.[2] As shown in the 3-dimensional AFM scan, the surface roughness of the Al_2O_3 film is very low in the range of ±1 nm. The smooth morphology with small surface roughness agrees with the amorphous nature of the film revealed by XRD. The profile scan in Fig. 8b reveals that the root mean square surface roughness is 0.52 nm for the 80-nm film.

The chemical composition of spray-deposited Al_2O_3 was evaluated by XPS. Fig. 9 shows an XPS spectrum of an 80-nm Al_2O_3 film. Only Al, O, and C are detected in the sample. The ratio of Al to O is 1:1.28, while stoichiometric Al_2O_3 has an Al to O ratio of 1:1.5. This suggests that spray-deposited Al_2O_3 is slightly Al rich and can be represented as Al_2O_{3-x}. A small amount of C, 5.5%, was detected by XPS, which is likely due to the organic precursor used in this work.

Fig. 10 compares the I-V characteristics of 80-nm spray-deposited Al_2O_3 and 10-nm ALD Al_2O_3/80-nm PECVD SiN_x. The substrates used for I-V were p-type polished CZ Si(100) wafers of 0.001 Ω-cm as the substrate serves as the bottom electrode in I-V characterization. Al dots with an area of 5.54×10^{-3} cm^2 were deposited on each sample by electron-beam evaporation. As shown in Table II, the resistivity and breakdown field of spray-deposited Al_2O_3 is 5.46×10^{14} Ω-cm and 3.28 MV/cm, respectively. These values are lower compared to the 10-nm ALD Al_2O_3/80-nm PECVD SiN_x stack but, considering that the open-circuit voltage of Si solar cells is about 0.7 V, the leakage current through 80-nm spray-deposited Al_2O_3 becomes negligible. To determine the thermal stability of the 80-nm spray-deposited Al_2O_3 film against high-temperature firing, these Al/Al_2O_3/Si samples were annealed at 800°C in a rapid thermal furnace for various durations.

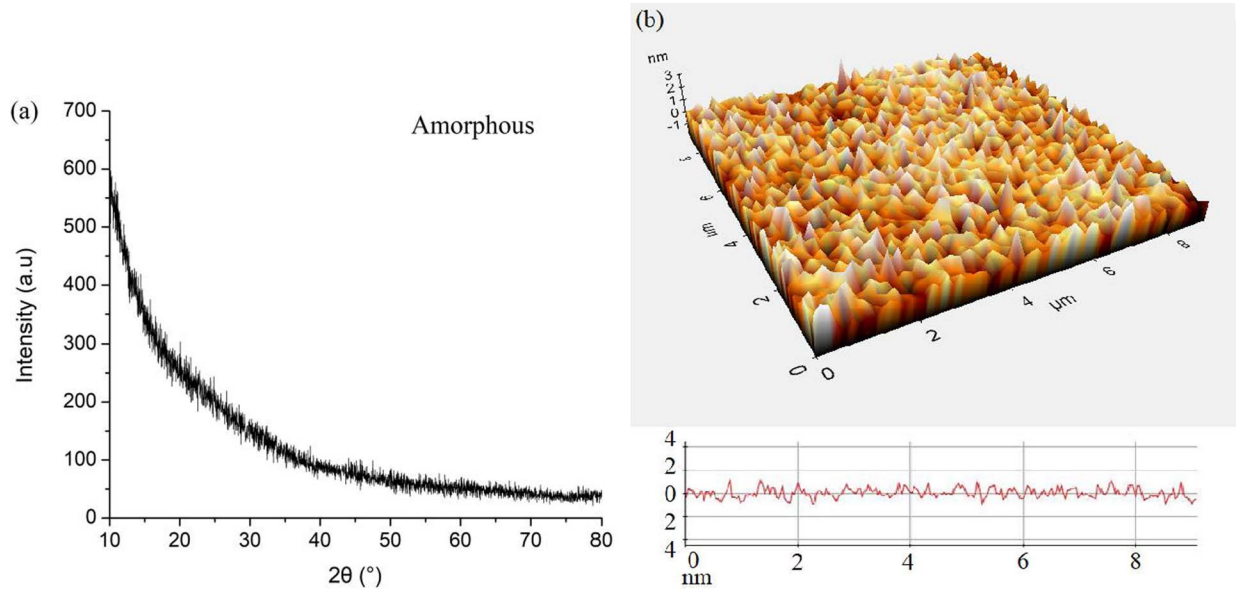

Figure 8. (a) XRD spectrum of a 500-nm Al_2O_3 film and (b) AFM image of an 80-nm Al_2O_3 film. Both films were deposited on polished Si(100) substrates at 550°C followed by post annealing in N_2 at 550°C for 1 hr.

It was found that the resistivity and breakdown field are stable after annealing at 800°C.

Conclusions

The possibility of using low-cost spray-deposited Al_2O_3 for rear passivation and optical trapping in Si PERC cells is investigated. Optical, electrical, and structural properties of spray-deposited Al_2O_3 films are examined and compared to the industrial standard ALD Al_2O_3/PECVD SiN_x stack. It was found that spray-deposited Al_2O_3 has a negative charge density of 3.19×10^{12} cm^{-2} for an 80-nm film, indicating that spray-deposited Al_2O_3 can serve as the passivation layer. Optical properties of spray-deposited Al_2O_3 are identical to the ALD Al_2O_3/PECVD SiN_x stack, suggesting that spray-deposited Al_2O_3 can also serve as the optical trapping layer. It was also found that spray-deposited Al_2O_3 is crack and pore free, and its surface roughness has a root-mean-square value of 0.52 nm for an 80-nm film. Spray-deposited Al_2O_3 is amorphous and its composition is slightly Al rich. The resistivity and breakdown field of 80-nm spray-deposited Al_2O_3 are 5.46×10^{14} Ω-cm and 3.28 MV/cm, respectively, which are stable after 800°C annealing. These properties suggest that spray-deposited Al_2O_3 is a promising candidate to replace the Al_2O_3/SiN_x stack in Si PERC cells.

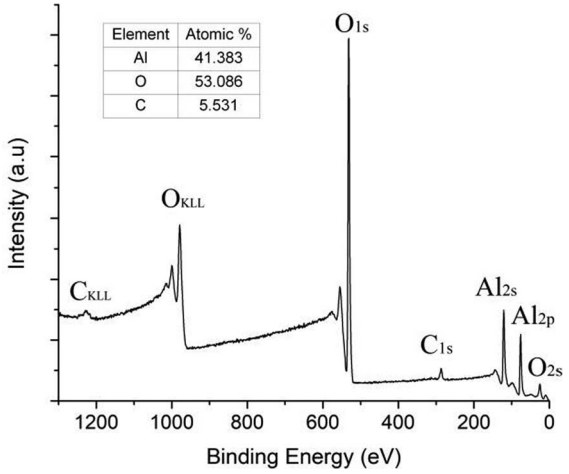

Figure 9. XPS spectrum of an 80-nm Al_2O_3 film deposited at 550°C on Si followed by post annealing in N_2 at 550°C for 1 hr.

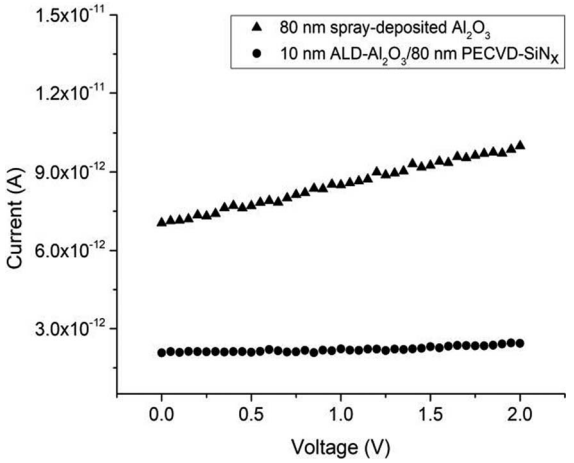

Figure 10. Comparison of I-V characteristics between an 80-nm spray-deposited Al_2O_3 film and a 10-nm ALD Al_2O_3/80-nm PECVD SiN_x stack.

Table II. Resistivity and breakdown field of 80-nm spray-deposited Al_2O_3 and 10-nm ALD Al_2O_3/80-nm PECVD SiN_x.

	Resistivity (Ω-cm)	Breakdown field (MV/cm)
80-nm spray-deposited Al_2O_3	5.46×10^{14}	3.28
10-nm ALD Al_2O_3/80-nm PECVD SiN_x	3.07×10^{15}	3.53

Acknowledgments

Financial support for this work was provided by the U.S. National Science Foundation under grant no. 1306542. WJS thanks Bill Dauksher for providing solar Si wafers and PECVD SiN_x deposition.

ORCID

Meng Tao https://orcid.org/0000-0001-5743-7092

References

1. A. Metz, D. Adler, S. Bagus, H. Blanke, M. Bothar, E. Brouwer, S. Dauwe, K. Dressler, R. Droessler, T. Droste, and M. Fiedler, *Sol. Energy Mater. Sol. Cells*, **120**, 417 (2014).
2. C. Roselund, International Technology Roadmap for Photovoltaic, International Technology Roadmap for Photovoltaic (7th edition, 2016).
3. N. Batra, J. Gope, R. Singh, J. Panigrahi, S. Tyagi, P. Pathi, S. K. Srivastava, C. M. S. Rauthan, and P. K. Singh, *Phys. Chem. Chem. Phys.*, **16**(39), 21804 (2014).
4. B. Vermang, H. Goverde, L. Tous, A. Lorenz, P. Choulat, J. Horzel, J. John, J. Poortmans, and R. Mertens, *Prog. Photovolt. Res. Appl.*, **20**(3), 269 (2012).
5. P. Saint-Cast, J. Haunschild, C. Schwab, E. Billot, M. Hofmann, J Rentsch, and R. Preu, *Energy Procedia*, **8**, 324 (2011).
6. M. D. Groner, F. H. Fabreguette, J. W. Elam, and S. M. George, *Chem. Mater.*, **16**(4), 639 (2004).
7. P. Saint-Cast, D. Kania, M. Hofmann, J. Benick, J. Rentsch, and R. Preu, *Appl. Phys. Lett.*, **95**, 151502 (2009).
8. C. E. Rice, J. D. Cuchiaro, S. Sun, L. G. Provost, G. S. Tompa, T. Davenport, G. Fox, S. Sun, and F. Chu, *Integ. Ferroelec.*, **59**(1), 1453 (2003).
9. H. J. Quah and K. Y. Cheong, *ACS Appl. Mater. Interfaces*, **5**(15), 6860 (2013).
10. J. Schmidt and M. Kerr, *Sol. Energy Mater. Sol. Cells*, **65**(1-4), 585 (2001).
11. H. Q. Xiao, C. L. Zhou, X. N. Cao, W. J. Wang, L. Zhao, H. L. Li, and H. W. Diao, *Chin. Phys. Lett.*, **26**(8), 088102 (2009).
12. S. Kalaivani and A. Kottantharayil, in *Conference Record of 42nd IEEE Photovoltaic Specialist* (New Orleans, LA, 2015), p. 1.
13. W. J. Shin, W. H. Huang, and M. Tao, *Mater. Chem. Phys.*, **230**, 37 (2019).
14. A. B. Sproul, *J. Appl. Phys.*, **76**(5), 2851 (1994).
15. A. W. Stephens and M. A. Green, *J. Appl. Phys.*, **74**(10), 6212 (1993).
16. M. Tao, *Terawatt Solar Photovoltaics Roadblocks and Opportunities*, p. 32, Springer, London, (2014).
17. G. Agostinelli, A. Delabie, P. Vitanov, Z. Alexieva, H. F. W. Dekkers, S. D. Wolf, and G. Beaucarne, *Sol. Energy Mater. Sol. Cells*, **90**(18-19), 3438 (2006).
18. R. Engel-Herbert, Y. Hwang, and S. Stemmer, *J. Appl. Phys.*, **108**(12), 124101 (2010).